The effect of silicon on the glass forming ability of the $Cu_{47}Ti_{34}Zr_{11}Ni_8$ bulk metallic glass forming alloy during processing of composites

H. Choi-Yim,[a] R. Busch, and W. L. Johnson
W.M. Keck Laboratory of Engineering Materials, 138-78, California Institute of Technology, Pasadena, California 91125

(Received 30 December 1997; accepted for publication 11 March 1998)

Composites of the $Cu_{47}Ti_{34}Zr_{11}Ni_8$ bulk metallic glass, reinforced with up to 30 vol % SiC particles are synthesized and characterized. Results based on x-ray diffraction, optical microscopy, scanning Auger microscopy, and differential scanning calorimetry (DSC) are presented. During processing of the composites, a TiC layer forms around the SiC particles and Si diffuses into the $Cu_{47}Ti_{34}Zr_{11}Ni_8$ matrix stabilizing the supercooled liquid against crystallization. The small Si addition between 0.5 and 1 at. % increases the attainable maximum thickness of glassy ingots from 4 mm for Cu–Ti–Zr–Ni alloys to 7 mm for Cu–Ti–Zr–Ni–Si alloys. DSC analyses show that neither the thermodynamics nor the kinetics of the alloy are affected significantly by the Si addition. This suggests that Si enhances the glass forming ability by chemically passivating impurities such as oxygen and carbon that cause heterogeneous nucleation in the melt. © *1998 American Institute of Physics.* [S0021-8979(98)00512-X]

I. INTRODUCTION

In recent years many bulk metallic glass forming alloys have been developed. These alloys include La–Al–Ni,[1] Zr–Al–Cu–Ni,[2] Zr–Ti–Cu–Ni–Be,[3] Zr–Ti–Cu–Ni,[4] or Zr–Ti (Nb)–Al–Cu–Ni.[5] Cooling rates of less than 100 K/s are sufficient to prevent nucleation and growth of crystals. Bulk metallic glasses (BMGs) have high yield strength and a high elastic strain limit combined with corrosion resistance, and relatively high fracture toughness.[6–9] However, the lack of tensile ductility limits the number of applications. One way to address this problem is to reinforce the glass. Recently it was shown that bulk metallic glass matrix composites reinforced by particles and wires could be processed successfully.[10,11] Those reinforcements include ceramics such as SiC, TiC, or WC. Ductility in compression and tension as well as fracture toughness was improved substantially by adding metallic particles and wires into the metallic glass. Metals like W and Ta were used.[12] Improvements of the mechanical properties are obtained by hindering propagation of shear bands and encouraging the formation of multiple shear bands due to the existence of the second solid crystalline phase.

Bulk metallic glass formers are excellent matrix materials for composites because of their low melting and glass transition temperatures. The low glass transition temperature helps to reduce differential thermal stresses, which develop between the reinforcement and matrix during freezing upon cooling. The low melting temperatures of metallic glass formers result in slow chemical interactions between the reinforcing particles and the liquid during processing. However, the dissolution or reaction of a certain amount of the reinforcement phase with the metallic glass matrix still has to be taken into account. These interfacial reactions and dissolution of reinforcement into the melt can be responsible for degradation of the glass forming ability of the matrix, e.g., by moving the composition of the liquid out of the optimum glass forming range.[13]

In this study, we observe the opposite case. One can improve the glass forming ability of the matrix by interdiffusion between the reinforcement and the metallic glass matrix. It will be shown that the addition of Si to the Cu–Ti–Zr–Ni alloy enlarges the supercooled liquid region and the glass forming ability.

II. EXPERIMENTAL METHODS

The $Cu_{47}Ti_{34}Zr_{11}Ni_8$ alloy (V101)[4] was used as a matrix material for composites. Ingots of the alloy were prepared by arc melting a mixture of the elements having a purity of 99.7 at. % or better. Subsequently a mixture of the prealloyed V101 and SiC particles was induction melted on a water cooled copper boat under a 800 mbar Ti-gettered argon atmosphere. Volume fractions of SiC particles ranged from 10% to 30% and the average size of the particles was 50 μm. In order to obtain an amorphous matrix, the composites were then cast into Cu molds. This resulted in rods with a diameter of 3 mm and a length of 30 mm. In addition, quintary $Cu_{47}Ti_{34-x}Zr_{11}Ni_8Si_x$ ($x=0.5$, 1, 2) alloys (V102) were synthesized. First, binary alloys were prepared by arc melting a mixture of Cu and Si to form a solid solution of Si in Cu. Then the binary Cu–Si solid solution and the other three elements were arc melted together under argon atmosphere. Ingots were remelted and cast into a copper mold resulting in glassy strips or rods of different sizes up to a dimension of 7 mm.

Cross sections of cast strips and rods were examined by x-ray diffraction. The particle distribution in the composite specimens was investigated by optical microscopy. In selected samples the interfaces between particles and matrix were examined by scanning Auger microscopy. The glass transition and crystallization of all samples was studied with

[a]Electronic mail: hchoi@cco.caltech.edu

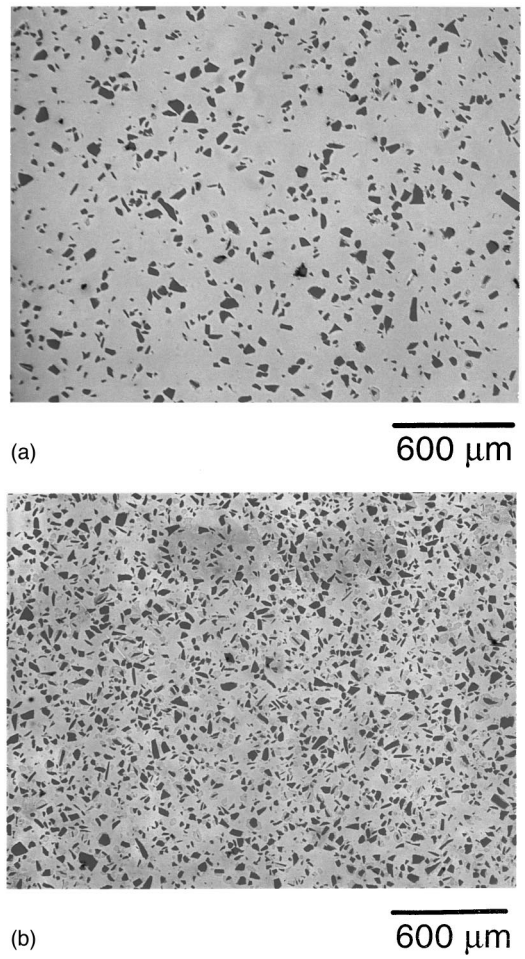

FIG. 1. Optical micrographs of $Cu_{47}Ti_{34}Zr_{11}Ni_8$, (V101)/SiC composites, showing the uniform distribution of SiC particles in the V101 matrix. In (a) the volume fraction of SiC particles is 10% and in (b) it is 20%. The average size of particles is about 50 μm.

a Perkin-Elmer differential scanning calorimeter (DSC) 7. Different heating rates between 0.0167 and 3.33 K/s were used. In addition, the melting behavior of the crystallized alloys was investigated in a Perkin–Elmer DTA 7.

III. RESULTS

Figure 1 shows the optical micrographs of the uniformly distributed SiC particles in the metallic matrix. The volume fractions of SiC particles are 10% and 20% in Figs. 1(a) and 1(b), respectively. The matrix appears uniform and free of heterogeneity. In Fig. 2 the x-ray diffraction patterns of the amorphous matrix, the composite, and the SiC particles are compared. The pattern of the specimen containing 30 vol %, SiC in a V101 matrix shows diffraction peaks of SiC particles superimposed on the broad diffuse scattering maxima from the amorphous phase. The positions of the peaks in Figs. 2(b) and 2(c) match exactly. However the intensity of the peaks are not the same due to the changing texture of the particles during processing. No other phases are detected within the sensitivity limits of x-ray diffraction. The volume

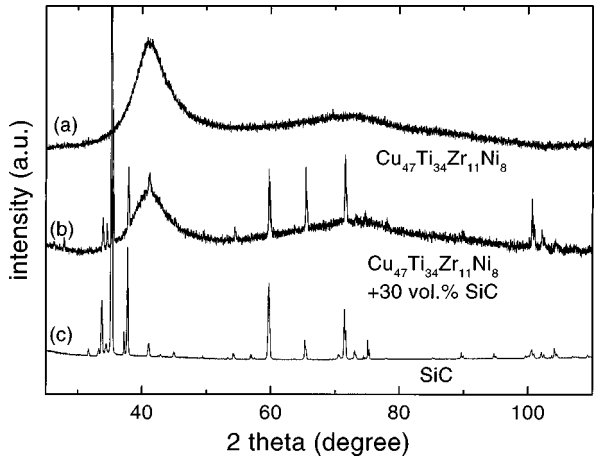

FIG. 2. X-ray diffraction patterns of (a) the amorphous $Cu_{47}Ti_{34}Zr_{11}Ni_8$, (b) a composite containing 30 vol % SiC, and (c) the pure SiC powder.

fraction of a thin TiC interlayer between the SiC particles and the glassy matrix (see below) is too small to be detected by x-ray diffraction.

The glass transition and the crystallization behavior of the amorphous matrix of the composites were investigated in DSC scans using various heating rates. Figure 3 shows DSC scans of the pure amorphous V101 and a series of SiC/V101 composites with increasing SiC volume fraction from 10 to 30 vol %. All measurements were performed with a heating rate of 0.33 K/s. They exhibit the endothermic heat effect due to the glass transition and the three characteristic steps of heat release, indicating the successive stepwise transformations from the metastable supercooled liquid state into the crystalline compounds. The glass transition temperature, T_g, is here defined as the onset of the endothermic DSC event. The primary crystallization temperature, T_{x1}, is defined as the onset temperature of the first exothermic event. Based on the DSC scans, it is observed that the addition of SiC particles into the V101 produces a significant extension of the supercooled liquid region (ΔT_x) defined by the difference

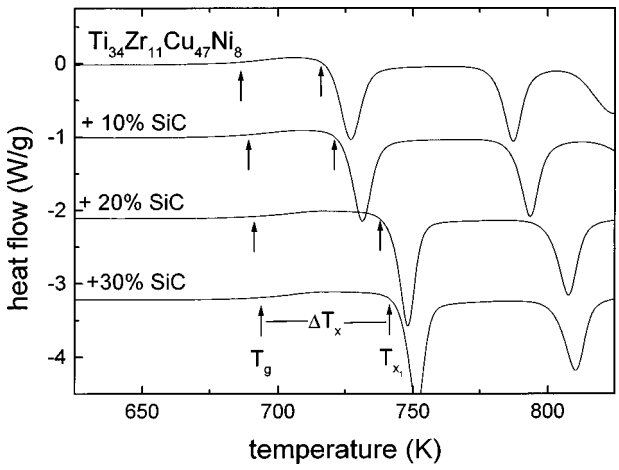

FIG. 3. DSC thermogram (heating rate of 0.33 K/s) of V101 and SiC reinforced V101 with a volume fraction of 10%, 20%, and 30%, respectively. The width of the supercooled liquid region, ΔT_x, between onset of the glass transition, T_g, and the onset of primary crystallization, T_{x1}, increases with rising SiC particle content. The average particle size is 50 μm.

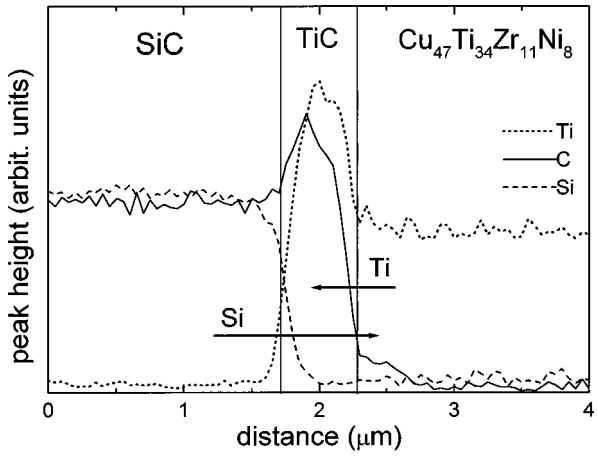

FIG. 4. Scanning Auger microscopy line scans across the V101/SiC interface. A TiC layer with a thickness of about 500 nm formed at the interface during processing when the V101 was in the liquid state.

between T_g and T_{x1}. With increasing SiC particle addition into V101, the glass transition temperature increases slightly. The onset temperature of primary crystallization (T_{x1}) rises even more, resulting in an increase of ΔT_x from 46 K in the pure V101 to 66 K for the V101 that was reinforced with 30 vol % SiC. This means that, surprisingly, the thermal stability of the bulk metallic glass matrix was enhanced during composite processing.

In order to investigate the reaction that must have taken place during reactive wetting of the SiC particles by the matrix, the composites were investigated by scanning Auger microscopy. Figure 4 shows the results of an Auger line scan across the interface between matrix and particle. The Auger signals for Si, C, and Ti are depicted. At the interface a TiC layer with a thickness of 500 nm has grown. It forms a shell around the SiC particles. This means during processing Ti must have diffused from the matrix into the TiC layer, whereas Si must have diffused from the SiC particle throughout the TiC layer into the melt. In first approximation the Si content of the matrix equals the reduction of the Ti content in the melt. These observations suggest that a Si addition to V101 is the reason for the enhanced thermal stability of the alloy.

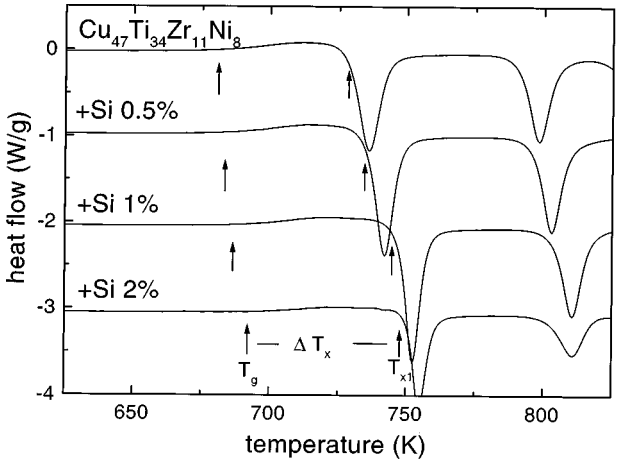

FIG. 5. DSC thermogram (heating rate of 0.33 K/s) of V101 and of the Si bearing alloys (V102).

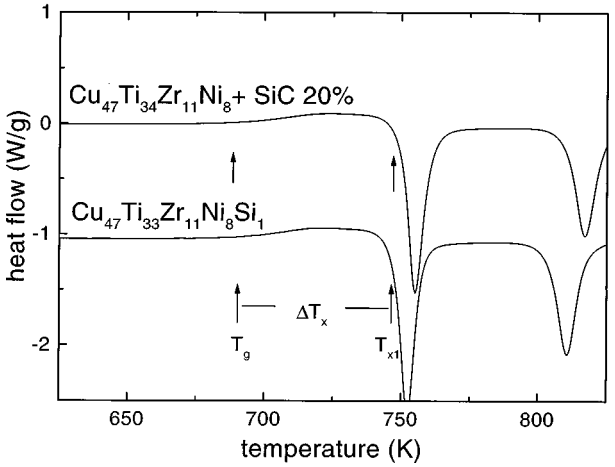

FIG. 6. DSC scans of the composite with a volume fraction of 20% particle in comparison with the $Cu_{47}Ti_{33}Zr_{11}Ni_8Si_1$, alloy of (0.33 K/s).

To prove this, we prepared alloys in which we substituted 0.5, 1, and 2 at. % of the Ti in V101 by Si. These concentrations can be estimated from the TiC layer thickness, the particle size, and volume fraction. They are the approximate matrix Si concentration in the composites containing 10, 20, and 30 vol % SiC, respectively. The DSC scans of these $Cu_{47}Ti_{34-x}Zr_{11}Ni_8Si_x$ alloys (V102) are shown in Fig. 5 in addition to the pure V101. The Si addition substantially increases the supercooled liquid region. As can be seen in Fig. 6, the DSC scan for a sample with 1% Si is in good agreement with the DSC scan of a composite with 20 vol % SiC. The matrix of the composite with a SiC content of 10 vol % contains 0.5 at. % Si (not shown).

The enlarged supercooled liquid region after Si addition suggests that the V102 alloys have a better glass forming ability than the V101 alloys, which we can mold cast up to a thickness of 4 mm. Figure 7 compares the DSC scans of cast samples of V101 with samples of V102 containing 0.5 and 1 at. % Si, respectively. The V101 alloy does not show a glass

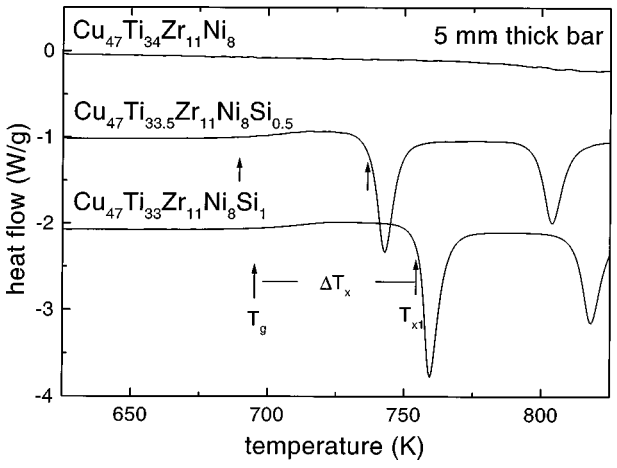

FIG. 7. DSC thermograms of V101 and two V102 alloys with different Si content, having dimension of 5 mm V101 was completely crystalline, whereas the V102 alloys were amorphous prior to the DSC measurements.

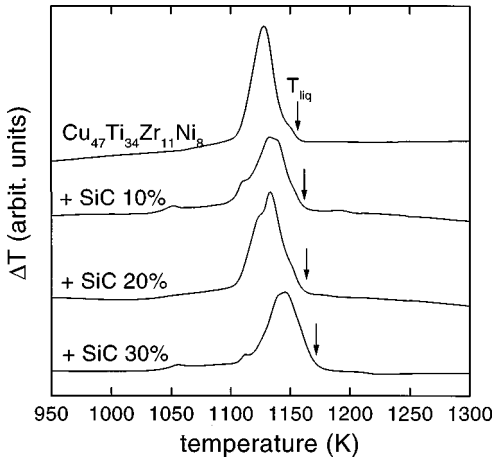

FIG. 8. DTA melting endotherms of the composites with different SiC contents. The liquidus temperatures of the matrix increase slightly with the Si content.

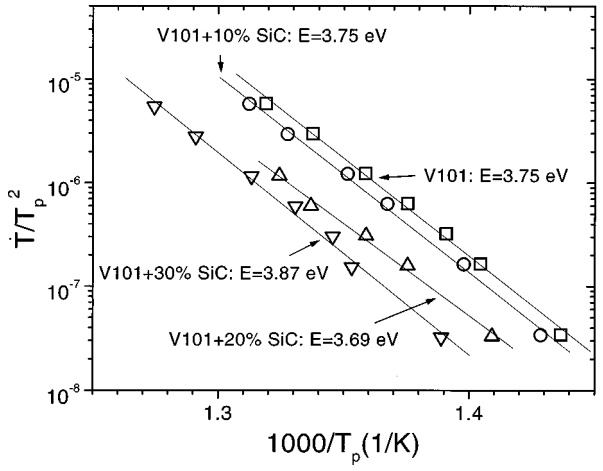

FIG. 9. Kissinger plots obtained after heating the composites with different heating rates. The activation energy for nucleation does not decrease if SiC particles are added. Heterogeneous nucleation at the interface between the TiC layer and the melt does not occur.

transition and crystallization peaks. It is completely crystalline. The V102 alloys, in contrast, are completely amorphous as additional x-ray diffraction investigations confirm. The alloy that contains 1 at. % Si could be cast up to a thickness of 7 mm, which is an improvement by a factor of 1.7 compared to V101. This reveals that the critical cooling rate for the Si-bearing alloy to form a glass is about a factor of 3 smaller than for the alloy without Si, because the critical thickness of the sample is approximately proportional to the square root of the critical cooling rate. If we increase the amount of Si to 2 at. % the glass forming ability degrades again, even though the supercooled liquid region becomes larger (Fig. 5). This is probably due to the fact that the formation of high melting point silicides could not be avoided during processing. These silicides are likely to serve as heterogeneous nucleation sites.

The addition of silicon to the alloy increases the glass transition temperature of the alloy slightly. The reduced glass transition temperature, T_{rg}, is a value to estimate the glass forming ability of alloys and represents the ratio of glass transition temperature and liquidus temperature. In order to determine whether the reduced glass transition temperature changes with Si content, the melting behavior of the different alloys was investigated. As Fig. 8 reveals, the liquidus temperature increases slightly with Si content, which compensates the effect of an increasing glass transition temperature. The reduced glass transition temperatures for all the alloys are 0.58 within the experimental error when heated with a rate of 0.33 K/s.

IV. DISCUSSION

During composite processing of SiC in a $Cu_{47}Ti_{34}Zr_{11}Ni_8$ bulk metallic glass matrix, we observed the formation of TiC at the interface between liquid matrix and solid SiC particles (Fig. 4). The growth of this layer is most likely diffusion controlled. It is governed by the diffusion of Ti from the matrix throughout the layer to the interface between the TiC and the SiC. Si diffuses in the opposite direction through the TiC layer and finally into the matrix. If one considers the high melting point of TiC of 3140 K we can assume that the growth of the TiC layer proceeds much slower than the diffusion of Si in the liquid matrix. This means that the Si becomes virtually evenly distributed in the matrix. The result is a homogeneous matrix with a Si composition that depends on the interface area between particles and matrix as well as on the thickness of the reacted Ti–C layer. The matrix is thermally more stable with respect to crystallization when heated above the glass transition than the $Cu_{47}Ti_{34}Zr_{11}Ni_8$ alloy without silicon.

The same thermal stability can be obtained by just alloying the appropriate amount of Si with the initial alloy. In fact, if we assume that we replace each Ti atom in the matrix that participated in the TiC formation by a Si atom, we calculate as well as find experimentally that the processing of 10 vol % 50 μm SiC particles results in a matrix concentration of 0.5 at. % Si. Consequently, an increase of volume fraction to 20% with same particle size results in 1 at. % Si in the matrix.

At this point the question arises how such a small amount of Si can improve the glass forming ability considerably. As mentioned above, the reduced glass transition temperature of the alloy is virtually independent of the Si concentration. Both the glass transition temperature and the liquidus temperature increase slightly. In addition the specific heat capacity difference at the glass transition as well as the entropy of fusion do not change. All these factors indicate that the thermodynamics of the alloy do not change by adding the silicon.

The calorimetric studies were used to calculate the activation energies of crystallization for the investigated SiC reinforced V101 composites. By measuring the peak positions in Fig. 3 at different heating rates, it is possible to determine the activation energies for the different reaction steps by the Kissinger method,[14] i.e., from the slopes of the curves of $\ln[(\partial T/\partial t)/T_p^2]$ against $1/T_p$, where T_p, is the peak temperature and $\partial T/\partial t$ the heating rate. These results are presented in Fig. 9 for V101 and SiC reinforced V101 composites. The plot reveals that there is no significant change in activation barrier when adding the SiC particles and introducing Si into

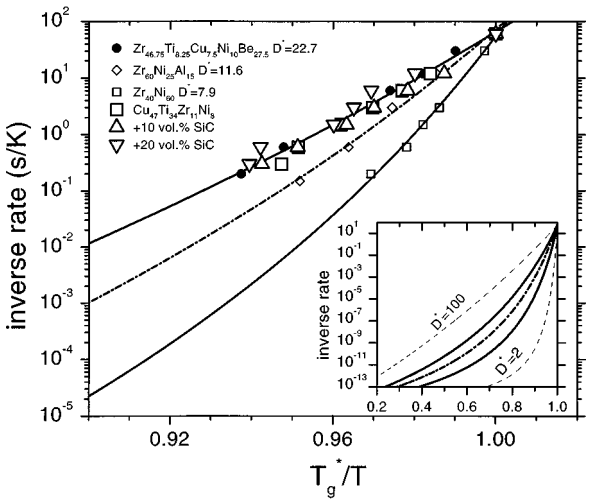

FIG. 10. Fragility plot of the inverse heating rate as a function of onset temperature for the glass transition normalized to the onset temperature of the glass transition measured with a rate of 0.0167 K/s (T_g). The kinetics of the glass transition do not change significantly with Si content. The inset (same units on the *x* axis) shows the range of structural relaxation times that are observed for different materials.

the glass matrix. This finding has two consequences. First, the interfaces between the TiC layer and the matrix do not act as heterogeneous nucleation sites, which would decrease the nucleation barrier. Second, the Si does not substantially change the growth kinetics and crystallization products. As shown in Fig. 3 the crystallization events are only shifted to higher temperatures.

The heating rate dependence of the glass transition can be analyzed by another method. It was shown earlier[15] that the heating rate dependence of T_g reflects the temperature dependence of the viscosity and the structural relaxation time in the supercooled liquid. Bulk metallic glasses are strong liquids[16] that show a pronounced heating rate dependence of the glass transition, which represents the structural relaxation. In Fig. 10, the inverse heating rate is plotted as a function of onset of glass transition normalized to T_g^*, which is the onset of the glass transition measured at 0.0167 K/s. On this ''fragility plot'' data are shown for different metallic glass formers. The parameter D^* indicated in Fig. 10 is a measure for the fragility of the liquid. As shown in the inset in Fig. 10, relaxation time curves for different materials are found between $D^*=100$ (strong) and $D^*=2$ (fragile).[17] Less complex alloys such as Zr–Ni or Zr–Al–Ni are more fragile (less strong) than Zr–Ti–Cu–Ni–Be or Cu–Ti–Zr–Ni–(Si). A high fragility means a fast increase of the structural relaxation time upon rising temperature. The strong Cu–Ti–Zr–Ni alloy shows a slow increase of the structural relaxation time. It can be seen in Fig. 10 that the introduction of Si into the Cu–Ti–Zr–Ni matrix does not change the fragility of the alloy, i.e., if we add 10 and 20 vol % SiC, respectively, Si does not affect the relaxation kinetics of the supercooled liquid. All Cu–Ti–Zr–Ni–(Si) liquids show the same fragility within the experimental error.

We thus can rule out that the Si influences the thermodynamics (reduced glass transition temperature), the crystallization kinetics (activation energy), and the intrinsic kinetics (structural relaxation time) in the supercooled liquid of the alloy.

V. CONCLUSIONS

Bulk amorphous $Cu_{47}Ti_{34}Zr_{11}Ni_8$ composites containing SiC particles up to 30 vol % were formed by copper mold casting. The interface reaction between particles and matrix resulted in the dissolution of Si into the matrix that enhanced the glass forming ability of the matrix even though the thermodynamic and kinetic properties of the matrix did not change considerably. This leads us to the conclusion that the Si most likely acts on the impurities in the melt predominantly present in the form of oxygen.

It was shown for the $Zr_{52.5}Ti_5Cu_{17.9}Ni_{14.6}Al_{10}$ alloy that an increasing amount of oxygen destroys the glass forming ability, which suggests that the presence of heterogeneous nucleation sites within the melt plays an important role during crystallization.[5] This effect should not be confused with heterogeneous nucleation at a particle/matrix interface. Since a certain amount of impurities cannot be avoided in the melt, it is desirable to neutralize the nucleation sites.

In the Ni–Pd–P alloy system it was shown by Volkert and Spaepen[18] that the addition of 1 at. % Si improves the thermal stability of the supercooled liquid of this particular alloy. In this case the improvement by adding Si was attributed to the destabilization of P_2O_5 clusters that were considered to act as nucleation sites. In our Ti based alloy the Si might act in a similar way. Si might help to destabilize TiO_2 clusters present in the melt.

ACKNOWLEDGMENTS

The authors would like to thank M. Tenhover for providing the scanning Auger microscope data. This work was jointly supported by U.S. Army Research Office, the Air Force Office of Scientific research under ARO Grant No. DAAH04-95-1-0233 and the U.S. Department of Energy (Grant No. DEFG-03-86ER45242).

[1] A. Inoue, T. Zhang, and T. Masumoto, Mater. Trans., JIM **31**, 425 (1990).
[2] T. Zhang, A. Inoue, and T. Masumoto, Mater. Trans., JIM **32**, 1005 (1991).
[3] A. Peker and W. L. Johnson, Appl. Phys. Lett. **63**, 2342 (1993).
[4] X. H. Lin and W. L. Johnson, J. Appl. Phys. **78**, 6514 (1995).
[5] X. H. Lin, Ph.D. thesis, California Institute of Technology, 1997; X. H. Lin and W. L. Johnson, Mater. Trans., JIM **38**, 475 (1997).
[6] H. A. Bruck, T. Christman, A. J. Rosakis, and W. L. Johnson, Scr. Metall. Mater. **30**, 429 (1994).
[7] H. A. Bruck, A. J. Rosakis, and W. L. Johnson, J. Mater. Res. **11**, 503 (1996).
[8] C. G. Gilbert, R. O. Ritchie, and W. L. Johnson, Appl. Phys. Lett. **71**, 476 (1997).
[9] D. Conner, A. J. Rosakis, and W. L. Johnson, Scr. Mater. **37**, 1373 (1997).
[10] H. Choi-Yim and W. L. Johnson, Appl. Phys. Lett. **71**, (1997).
[11] R. B. Dandliker, R. D. Conner, and W. L. Johnson, J. Mater. Res. (in press).
[12] D. Conner, Ph.D. thesis, California Institute of Technology, 1997.
[13] R. B. Dandliker, Ph.D. thesis, California Institute of Technology, 1997.
[14] H. E. Kissinger, Anal. Chem. **29**, 1702 (1957).
[15] R. Busch, W. Liu, and W. L. Johnson, J. Appl. Phys. **83**, 4134 (1998).
[16] R. Busch, A. Masuhr, E. Bakke, and W. L. Johnson, Mater. Res. Soc. Symp. Proc. **455**, 369 (1997).
[17] C. A. Angell, Science **267**, 1924 (1995).
[18] C. A. Volkert, Ph.D. thesis, Harvard University, 1988.